## RESEARCH ARTICLE

**Correspondence to:**
C. van der Tol,
c.vandertol@utwente.nl

# Models of fluorescence and photosynthesis for interpreting measurements of solar-induced chlorophyll fluorescence

C. van der Tol[1], J. A. Berry[2], P. K. E. Campbell[3], and U. Rascher[4]

[1]Department of Water Resources, Faculty ITC, University of Twente, Enschede, Netherlands, [2]Department of Global Ecology, Carnegie Institution of Washington, Stanford, California, USA, [3]Joint Center for Environmental Technology, University of Maryland, Baltimore County, Baltimore, Maryland, USA, [4]Institute of Bio- and Geosciences, IBG-2: Plant Sciences, Forschungszentrum Jülich GmbH, Jülich, Germany

**Abstract** We have extended a conventional photosynthesis model to simulate field and laboratory measurements of chlorophyll fluorescence at the leaf scale. The fluorescence paramaterization is based on a close nonlinear relationship between the relative light saturation of photosynthesis and nonradiative energy dissipation in plants of different species. This relationship diverged only among examined data sets under stressed (strongly light saturated) conditions, possibly caused by differences in xanthophyll pigment concentrations. The relationship was quantified after analyzing data sets of pulse amplitude modulated measurements of chlorophyll fluorescence and gas exchange of leaves of different species exposed to different levels of light, $CO_2$, temperature, nitrogen fertilization treatments, and drought. We used this relationship in a photosynthesis model. The coupled model enabled us to quantify the relationships between steady state chlorophyll fluorescence yield, electron transport rate, and photosynthesis in leaves under different environmental conditions.

## 1. Introduction

During photosynthesis, part of the solar radiation absorbed by chlorophyll is reemitted at longer wavelengths (fluorescence). In plants, chlorophyll fluorescence can be considered as an unavoidable leak in the energy processing in photosystems [*Fleming et al.*, 2012], a process that is otherwise very efficient [*Mohseni et al.*, 2008; *Rebentrost et al.*, 2009; *Hildner et al.*, 2013]. Typically, less than 5% of absorbed photons are reemitted by plants as fluorescence. Although the reemission is a physical process, it is regulated by the biology of living cells. By measuring fluorescence, one can diagnose aspects of this regulation and assess the efficiency of the exciton use by photosystems.

Active measurements of fluorescence with dedicated, laboratory, and portable instruments have been used to assess the status of the photosynthetic apparatus in terrestrial plants for several decades [*Bilger et al.*, 1995]. Such measurements make it possible to quantify the probability of each of the three alternative fates of absorbed photons in the pigment bed: photochemistry, heat dissipation, and fluorescence [*Kitajima and Butler*, 1975; *Genty et al.*, 1989]. These measurements, in combination with measurements of gas exchange between leaves and the atmosphere, have lead to substantially improved knowledge of the process of photosynthesis [*Papageorgiou et al.*, 2004; *Porcar-Castell et al.*, 2014] and to a quantitative basis for relating fluorescence measurements to the rate of electron transport [*Butler*, 1978; *Weis and Berry*, 1987a; *Genty et al.*, 1989; *Loriaux et al.*, 2013].

The detection of solar-induced fluorescence (SIF) has more recently become feasible too. The detection of SIF requires instruments of high spectral resolution and high accuracy due to the fact that the weak fluorescence light has to be differentiated from the much stronger reflected ambient light (for a review of techniques, see *Meroni et al.* [2009]). An advantage of SIF is that the technique does not have limitations imposed by the strength of an artificial excitation source. During the last decade and especially in the 2010s, field measurements [*Moya et al.*, 2004; *Mazzoni et al.*, 2012], airborne measurements [*Guanter et al.*, 2007; *Zarco-Tejada et al.*, 2013], and spaceborne measurements [*Frankenberg et al.*, 2011; *Joiner et al.*, 2011] have been developed.

Triggered by the increase in SIF measurements, we are interested in characterizing the sensitivity of steady state fluorescence to physiological and biophysical states of the vegetation and in being able to simulate
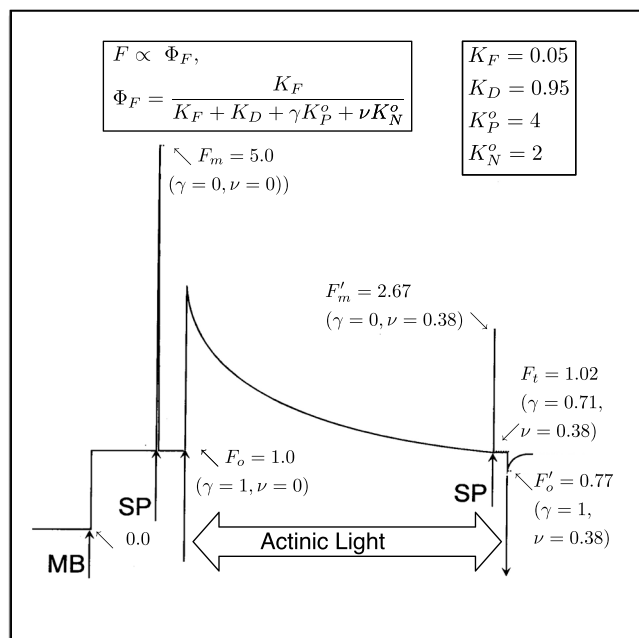
**Figure 1.** A sample trace of a measurement of fluorescence from a leaf with a PAM fluorometer [after *Maxwell and Johnson*, 2000]. The measuring light is turned on at MB; saturating pulses (1 s) are applied at SP. Note that $\gamma \to 0$ during a SP while $\nu$ is unchanged. The experiment shows changes in fluorescence that occur when actinic light is provided. The fluorescence levels ($F$) are normalized to the $F_o$ level. The photochemical yield of the leaf under dark adapted conditions $\Phi_P^o = (F_m - F_o)/F_m = (5.0 - 1.0)/5.0 = 0.8$ and after a period of illumination $\Phi_P = (F_m' - F_t)/F_m' = 0.62$. These arbitrary fluorescence levels can be related to absolute yields with the equations and probability constants shown in the boxes and the values of $\gamma$ and $\nu$. We used equations (8) and (9) to estimate $K_N$ and $K_P$, respectively, and $\gamma = K_P/K_P^o$ and $\nu = K_n/K_N^o$.

steady state fluorescence as an output of a photosynthesis model [e.g., *van der Tol et al.*, 2009a]. The degree to which SIF can be coupled to photosynthesis determines the opportunities we have for using it in carbon cycle models.

To achieve these goals, we need to dive down into the mechanisms of light harvesting and photon processing in the reaction centers of higher plants. In this study we will draw upon measurements conducted in a laboratory setting in which photosynthesis measurements by $CO_2$ exchange were combined with fluorescence, using the pulse amplitude modulation (PAM) measuring principle. This provides a highly selective measure of the relative chlorophyll fluorescence quantum yield. In conjunction with the saturating pulse method, PAM fluorometers allow assessment of photosynthetic energy conversion—information that we will need to build an understanding of remote sensing observations.

## 2. Theoretical Background

In this paper we distinguish fluorescence levels as measured with a PAM, with the symbol $F$ (Figure 1), coefficients for probabilities of excitons to follow a certain pathway with $K$, or quantum yields with $\Phi$. We use in subscripts the symbols P for photochemistry and D and N for heat dissipation, a constitutive thermal dissipation (D) that is present in dark adapted plants and a variable, energy-dependent heat dissipation (N) controlled by mechanisms that regulate the electron transport of the photosystems. Although this differentiation into two terms is only a simplified view, it is sufficient for our purpose and it prevents equifinality of the model.

An example of measurements of a leaf with a PAM fluorometer is illustrated in Figure 1. At the start (left), the leaf which has been in the dark for some time is illuminated by a dim beam of modulated light from a light-emitting diode (MB). The fluorescence elicited is also modulated and can be selectively detected by a special circuit. Application of an $\approx 1$ s pulse of unmodulated light more than sufficient to saturate photosynthesis, a so called saturating pulse (SP), will elicit a large pulse of fluorescence, but the detector sees only the effect of that light on the yield of fluorescence from the constant modulated light. This yield goes up several fold because the added light results in nearly complete closure of the PSII reaction centers ($\gamma \to 0$), blocking the photochemical deexcitation pathway and increasing the lifetime of the excitation. The level of fluorescence with only the measuring light is termed the $F_o$ level. The peak level of fluorescence that is reached during the pulse is termed $F_m$. Since the information from PAM experiments is contained in the ratio of the fluorescence levels rather than in the absolute power, the signals are generally normalized to $F_o = 1$ or $F_m = 5.0$ (Figure 1). The variable component of fluorescence ($F_v/F_m = (F_m - F_o)/F_m$) is related to the efficiency of photochemical trapping in the dark adapted state $\Phi_P^o = F_v/F_m$ when the traps are fully open [*Butler*, 1978]. This ratio is typically about 0.8 and is very similar among healthy plants [*Björkman and Demmig*, 1987].

In the next manipulation (Figure 1), a constant actinic light of an intensity sufficient to drive photosynthesis is turned on. This also elicits an increase in fluorescence, but this level, $F_t$, varies with time as the levels of photochemical and nonphotochemical tapping change in response to metabolic feedback processes, eventually reaching a steady state after several minutes. Applying a saturation pulse at this point results in a new, lower maximum fluorescence (2.67 in the example of Figure 1). To distinguish this from the dark adapted state, it is designated as $F'_m$. Turning all light except the measuring light off yields a new lower minimum $F'_o = 0.77$. The fact that the fluorescence level under steady state illumination $F_t$ is higher than $F'_o$ and lower than $F'_m$ indicates that in steady state some of the photochemical traps were closed. However, the levels $F'_m$ and $F'_o$ are substantially lower than their dark adapted values. This SP measurement takes advantage of the property that nonphotochemical traps do not change during the 1 s pulse, but the photochemical traps can be nearly completely closed by the pulse. This difference in relaxation time makes it possible to use PAM fluorometry to distinguish and evaluate the two types of trapping [*Weis and Berry*, 1987a] on the processing of excitations at $F_t$.

Bernard Genty, Jean-Marie Briantais, and Neil R. Baker [*Genty et al.*, 1989] proposed in highly cited paper that $\Phi_P$ at the steady state could be calculated from the ratio of the variable to the total fluorescence ($\Phi_P = (F'_m - F_t)/F'_m$). This is a very important concept as it makes it possible to use fluorescence and knowledge of the flux of photosynthetically active radiation (PAR) that is absorbed ($J_{aPAR}$) to estimate the rate of photosynthetic electron transport ($J_e$).

$$J_e = \Phi_P \cdot J_{aPAR} \tag{1}$$

While this equality portends great promise for using fluorescence to measure photosynthetic rate, it is important to note that most of the information is in the $F'_m$ level. $F_t$ is very similar to the $F_o$ level, yet $\Phi_P$ at the steady state is substantially lower than in the dark adapted state (0.62 versus 0.8). Observations of SIF will only see the steady state level. Information on $F'_m$ is beyond the reach of the method. We will show that there are significant, albeit small, changes in the $F_t$ level that can be related to photosynthetic rate.

Here we are finally interested in understanding the absolute yield of fluorescence, while PAM measurements are only concerned with the ratio of the levels. To make this transition, we adopt a formalism developed by *Butler* [1978] of using rate coefficients ($K$) to express the probability of the different fates of the excitations. The yields expressed with rate coefficients $K$ as follows:

$$\Phi_P = K_P / \sum K \tag{2}$$

$$\Phi_F = K_F / \sum K \tag{3}$$

$$\Phi_D = K_D / \sum K \tag{4}$$

$$\Phi_N = K_N / \sum K \tag{5}$$

$$\sum K = K_P + K_F + K_D + K_N. \tag{6}$$

Because they are mutually exclusive, the sum of the yields of all processes is unity

$$\Phi_P + \Phi_F + \Phi_D + \Phi_N = 1 \tag{7}$$

Because of the normalization by $\sum K$, the coefficients $K$ are unitless and can all be multiplied by the same scalar without any effect on the yields. The values used here ($K_D = 0.95$ and $K_F = 0.05$) have the useful property that $K_N \equiv$ NPQ (nonphotochemical quenching), a commonly reported parameter obtained from PAM fluorometry. The rate coefficients $K_N$ and $K_P$ vary with the metabolic state, and we will define these by reference to their respective maximum values. Thus, $K_P = \gamma K_P^o$ and $K_N = \nu K_N^o$. $K_P^o \approx 4$ and (as we will show later) $K_N^o$ varies from about 2 to 6 depending on the stress history of the vegetation. These dynamically changing rate coefficients for NPQ and for photochemistry $K_N$ and $K_P$ can be calculated as follows:

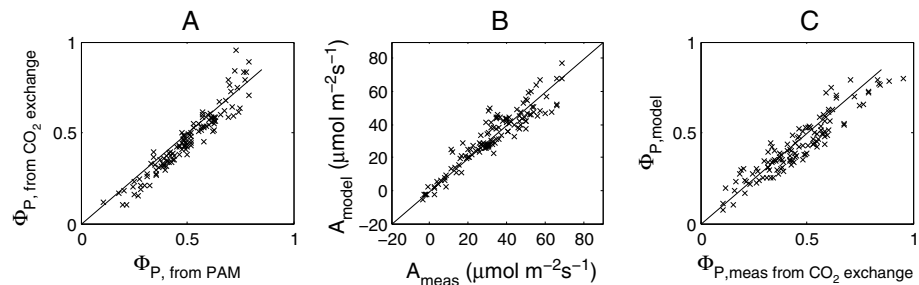$$K_N = \left( \frac{F_m}{F'_m} - 1 \right) (K_F + K_D) \tag{8}$$

**Figure 2.** Cotton data of (a) photochemical yield $\Phi_P$ from gas exchange versus $\Phi_P$ from PAM, (b) modeled [*Collatz et al.*, 1991] versus measured photosynthesis, and (c) modeled versus measured (from gas exchange) $\Phi_P$.

$$K_P = \left( \frac{F'_m}{F_t} - 1 \right)(K_F + K_D + K_N) \tag{9}$$

These equations have been derived from equations (2) to (6) using that $K_P$ is (by definition) zero at $F'_m$ and at $F_m$ and that $K_N$ is zero at $F_m$. These transformations are also illustrated in Figure 1.

An additional constraint on this system is that the flux of electrons produced by PSII photochemistry must equal the rate of reactions which consume electrons, and thus, $\Phi_P$ is constrained by the rate of $CO_2$ fixation. In equation (1) we already mentioned that

$$\Phi_P = J_e / J_{aPAR}. \tag{10}$$

The rate of electron transport $J_e$ in this equation can be obtained from the rate of gross $CO_2$ assimilation, $J_A$ (corrected for dark respiration), as follows:

$$J_e = 4J_A \frac{C_c + 2\Gamma*}{C_c - \Gamma*} \tag{11}$$

where $\Gamma*$ is the $CO_2$ compensation point and $C_c$ is the chloroplast $CO_2$ partial pressure estimated from gas exchange. The ratio on the right-hand side of equation (11) corrects for the effect that photorespiration, the competition of $O_2$ with $CO_2$, has on the stoichiometry linking $J_e$ to photosynthesis. Equation (11) bridges $CO_2$ gas exchange through stomata and cell walls with the photochemical electron transport. Following the assumption of *Farquhar et al.* [1980] feedback on $\Phi_P$ should be small when the energy supply for photosynthesis is limiting, for example, at low irradiance levels. As illumination increases, other factors such as resistance to $CO_2$ diffusion into the mesophyll or Rubisco limit the rate of photosynthesis and $\Phi_P$ becomes the dependent variable, and regulatory sequences [*Woodrow and Berry*, 1988] should limit the probability of photochemistry to maintain the equality of source and sink. This can occur in two ways: (a) by simple mass action when reduced electron carriers backup causing the photosystems to accumulate in the reduced (in active) form ($\gamma \downarrow$) or (b) by opening competing nonphotochemical traps ($v \uparrow$). It is thought that the pH gradient across the chloroplast membrane increases when turnover of the energy carrier adenosine triphosphate (ATP) becomes restricted and the reduced pH activates nonphotochemical traps. The change in the pH is also responsible for the conversion of violaxanthin into zeaxanthin, an effective nonphotochemical quencher of the excitons [*Gilmore*, 1997]. The mechanisms of NPQ and the their regulation are still an area of active research (for reviews, see *Ruban et al.* [2012] and *Zaks et al.* [2013]).

## 3. A Model for $\Phi_{F_t}$

All else being equal closure of photochemical traps will cause $\Phi_{F_t}$ to increase, and opening of nonphotochemical traps will cause $\Phi_{F_t}$ to decrease, yet both will have the effect of causing $\Phi_P$ to decrease. Regardless of the mechanism, however, the yield should follow the Genty relationship,
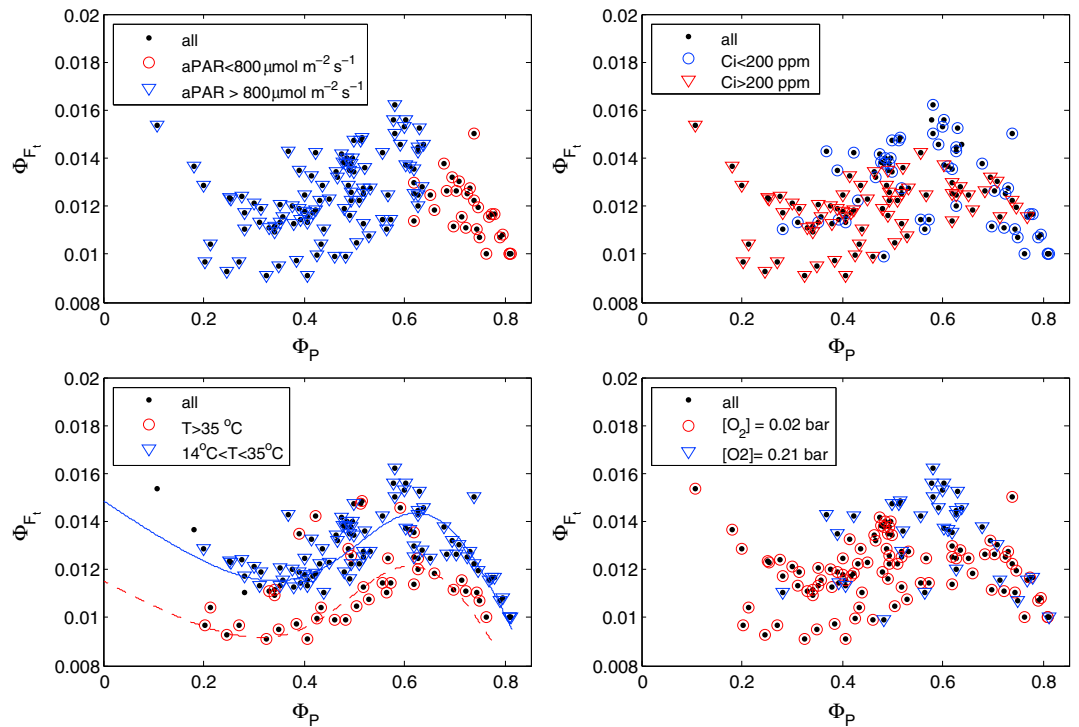
$$\Phi_{F_t} = (1 - \Phi_P)\Phi_{F'_m}. \tag{12}$$

**Figure 3.** The data and model results of the cotton experiment presented as $\Phi_{F_t}$ versus $\Phi_P$, with different symbols for driving variables. The lines are computed from the empirical $K_N(x)$ with temperature correction for 25°C (solid line) and 35°C (dashed line).

Here we will assume that we can know $\Phi_P$ independently, for example, from a photosynthesis model. Our next step is to find an independent approach to evaluate $\Phi_{F'_m}$. Following equation (3) and recalling that $K_P \to 0$ in SP , one may write that

$$\Phi_{F'_m} = \frac{K_F}{K_F + K_D + K_N} \tag{13}$$

in which only $K_N$ is unknown. While there is no theoretical basis to constrain $K_N$, we have sought an empirical relationship to relate $K_N$ to changes in $\Phi_P$. The central point of our approach is therefore to relate $K_N$ which controls $F'_m$ to the relative decrease in the yield of photochemistry. To quantify the strength of the feedback, we define a factor $x$ on a scale of 0 (photochemistry operating at full efficiency) to 1 (photochemistry totally blocked by feedback), $x$ is defined as follows:

$$x = 1 - \Phi_{J_e}/\Phi_{J_e}^o \tag{14}$$

where $\Phi_{J_e}$ is the quantum yield for electron transport linked to $CO_2$ fixation at steady state and $\Phi_{J_e}^o$ in the limit as $J_{aPAR} \to 0$. This is equivalent to

$$x = 1 - \frac{\Phi_P}{\Phi_P^o} \tag{15}$$

or, alternatively, after normalization of the fluxes by $aPAR$

$$\Phi_P = (1 - x)\Phi_P^o \tag{16}$$

where $\Phi_P^o$ is the maximum photochemical yield as observed under dark adapted, low light conditions. Substituting equation (16) into equation (12) results in the following:

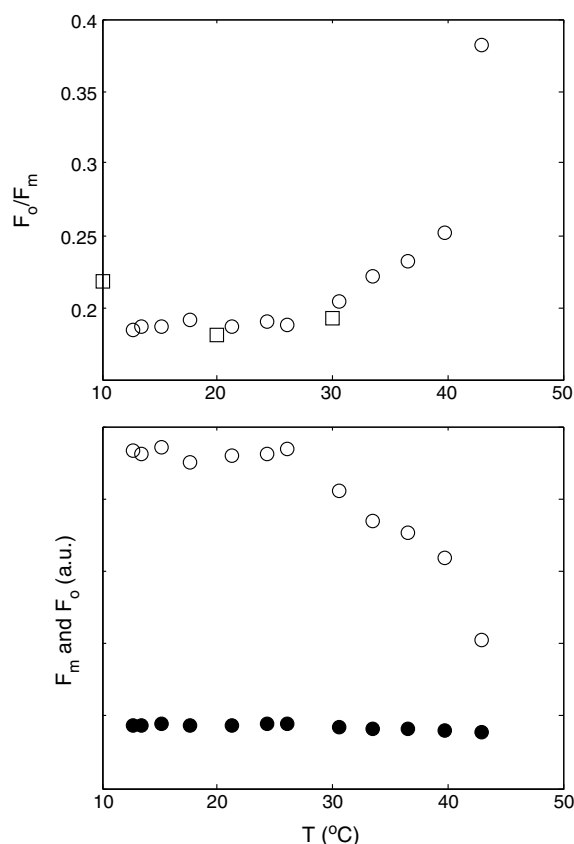$$\Phi_{F_t} = (1 - \Phi_P^o + x\Phi_P^o)\Phi_{F'_m} \tag{17}$$

**Figure 4.** (top) Measurements of $F_o/F_m$ at different temperatures for the cotton experiment (circles) and the tobacco experiment (squares). (bottom) $F_m$ (open symbols) and $F_o$ (closed symbols) at different temperature for the cotton experiment. Note that the values are relative, and the unit on the y axis is arbitrary

The aim here is to assess to what extent a general relationship $\Phi_{F'_m} = f(x)$ exists that can substitute $\Phi_{F'_m}$ in this equation, thus enabling the modeling of steady state fluorescence from a gas exchange measurement or vice versa. We used a collection of PAM data sets to assess this further. Our strategy is to make use of a large comprehensive data set obtained with cotton to develop a modeling approach and then to extend the analysis to other data sets that span different species, different environmental conditions, and different photosynthetic types. These additional data sets provided an opportunity to test our model and obtain additional information useful to make our model more general.

## 4. Data Description

Four sets of measurements with a PAM fluorescence sensor [*Schreiber et al.*, 1986] in combination with a leaf gas exchange chamber were used. The data sets were chosen to represent variations in the main driving variables. Three data sets concerned light and $CO_2$ response curves (cotton, tobacco, and maize), two of these had additional measurements at different temperatures and one at different nitrogen fertilization. Measured $C_i$ [*LI-COR Biosciences Inc.* 2004] rather than $C_c$ (equation (14)) was used to calculate $J_e$ lacking measurements of mesophyll conductance in these studies. Also, note that all of the active fluorescence measurements were made using a single-intensity saturating flash. The resulting values for $F_m$ and $F'_m$ might be underestimated in this way [*Markgraf and J. Berry*, 1990]. A recent paper [*Loriaux et al.*, 2013] suggests an alternative method for measurement. We have not evaluated the impact of this alternative method on our analysis. Another limitation of our study is that the broadband active fluorescence data include a portion of photosystem I (PSI) [*Franck et al.*, 2002]. In order to estimate the PSI contribution accurately, we would need to account for wavelength and leaf structure dependent reabsorption of the emitted fluorescence in the leaf (because PSI and PSII emit at different wavelengths and the PAM detector is sensitive to a part of the fluorescence spectrum that overlaps with the chlorophyll absorption spectrum). Because we did not have concurrent spectrometry data, we decided not to correct for the PSI fraction in this study but to use the measurements as they are instead. The fluorescence yields thus refer to the total fluorescence of both photosystems. C4 species have a slightly larger PSI contribution [*Genty et al.*, 1989]. We intend to address the separation of PSI and PSII fluorescence by incorporating spectral measurements and a radiative transfer model for the leaf in a separate study.

### 4.1. Cotton Data Set

This data set consists of measurements on cotton leaves over a temperature range from 14 to 40°C, including light responses, $CO_2$ responses, and measurements at low (to minimize photorespiration) and normal $O_2$ concentration. The experiment is described in *Weis and Berry* [1987b]. The original measurements, which were normalized to an $F_m$, were rescaled to fluorescence data normalized to $F_o$. Gas exchange measurements were taken simultaneously.
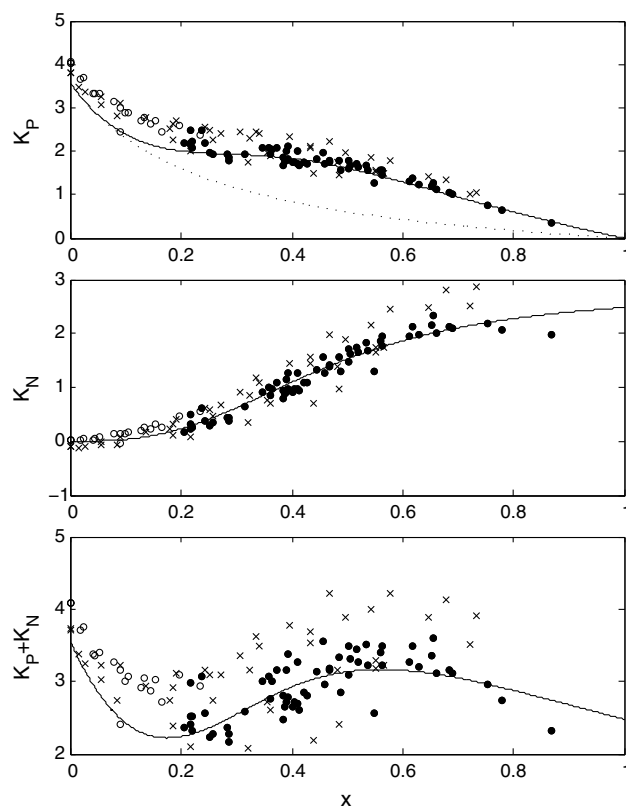
**Figure 5.** (top to bottom) Rate coefficients $K_P$ and $K_N$ versus relative light saturation of photosynthesis $x$, calculated from active fluorescence measurements of for cotton leaves exposed to varying irradiance, varying $CO_2$ concentration, and varying temperature. Open symbols refer to low light conditions ($Q < 800$ μmol m$^{-2}$ s$^{-2}$), crosses to high-temperature data ($T > 35°C$), and closed symbols to all other data. The solid line is an empirical model fit, and the dotted line is the theoretical value for $K_P$ if $K_N$ were always zero.

### 4.2. Tobacco Data Set

We used unpublished experimental data of greenhouse grown *Nicotiana tabacum* plants collected by A. Moersch at the Forschungszentrum Jülich in 2009. Measurements were carried out on attached leaves in a climatized cuvette under three leaf temperature regimes, 10, 20, and 30°C, with relative humidity of 94, 86, and 77% for the respective treatments. Gas exchange was measured with a CMS-400 gas exchange measurement system (Walz, Germany), concurrent with Mini-PAM fluorescence (Walz, Germany). Reflectance, water content, specific mass, and pigment composition were measured as well, but these data are not considered in the present study. The measurement sequence was as follows. A single leaf was clamped in a dark leaf cuvette, while gas exchange was measured continuously. After 30 min of acclimation, the gas exchange measurements were recorded, and $F_o$ and $F_m$ measurements were taken with the Mini-PAM. The measurements were repeated at light intensities of 77, 165, 310, 561, and 1051 μmol m$^{-2}$s$^{-1}$, each time after 30 min of acclimation. The whole measurement sequence was repeated 5 times in a period of 20 days but with the light intensity changes in a variable order (always starting with a dark adapted measurement).

### 4.3. Drought Stress of Several Species

Data published by *Flexas et al.* [2002] of the following C3 species were used: *Vitis vinifera L* (grape) in the field, *Solanum melongena L.* plants (herbaceous crop), 5 year old plants of *Quercus ilex L.* (evergreen sclerophyll tree), *Pistacia terebinthus L.* (deciduous sclerophyll shrub), and *Celtis australis L.* (deciduous mesophyte tree) grown in large pots. Measurements included combined leaf gas exchange (LI-6400) and fluorescence (PAM-2000) under saturating light [*Flexas et al.*, 1998]. After daily irrigation, the plants were subjected to progressive drought stress. Measurements of $F_o$ and $F_m$ (after acclimation to a dark room in the morning) and $F'_m$ and $F_t$ at full sunlight were taken every other day for 3 weeks.

### 4.4. Maize Data Set

In August 2013, as a part of a field measurement campaign supporting the collaborative NASA/U.S. Department of Agriculture (USDA) project "Spectral Bio-Indicators of Ecosystem Photosynthetic Efficiency II: Synthesis and Integration" (PI Dr. E. Middleton), we collected simultaneously leaf gas exchange parameters and active fluorescence light and $CO_2$ response curves on maize (*Zea mays, L.*) at the irrigated Replicated Nitrogen (N) research plots of the Optimizing Production inputs for Economic and Environmental Enhancement (OPE3) site, USDA Beltsville Agricultural Research Center, Beltsville, MD. At OPE3, adapted maize hybrids are planted in 0.76 m rows on the predominately loamy sand soils and grown under four fertilizer rates (0, 50, 100, and 150% of the recommended rates for these soils), following locally optimized management practices [*Daughtry*, 2001]. Irrigation timing and amounts are determined using soil moisture
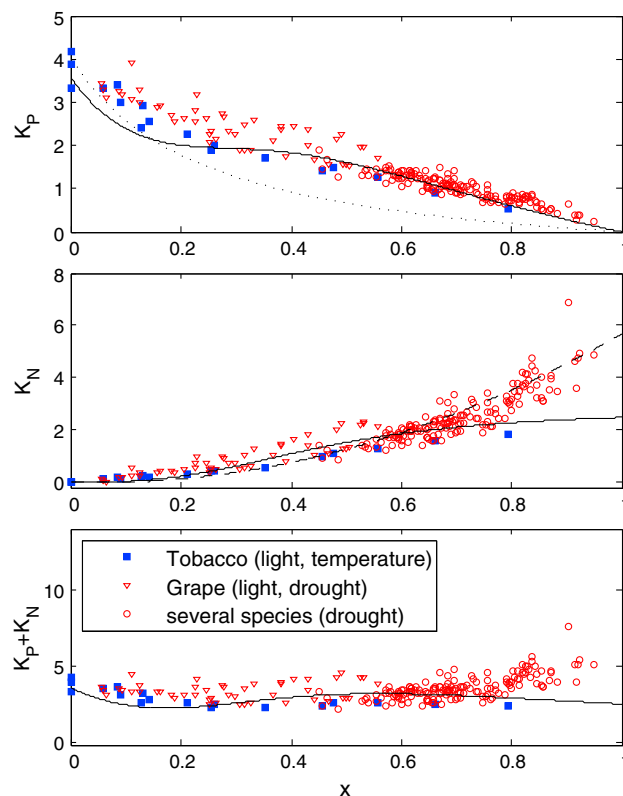
**Figure 6.** Similar to Figure 5 but for the other experiments: (1) tobacco leaves under different temperature and illumination and (2) grape and other C3 species subject to a drought experiment under full sunlight. The solid line represents the empirical fit of the cotton experiment, and the dashed line is calibrated to the drought experiment data.

sensors and adjusted to ensure the prevention of drought stress, providing a compact site ideally suited for the study of the effects of nitrogen on photosynthetic function and the associated vegetation spectral properties. Leaf gas exchange (assimilated net photosynthetic $CO_2$) and light and $CO_2$ response curves were collected, following standard procedures [*LI-COR Biosciences Inc.* 2004] on two consecutive days, from three plants representative of each N treatment ($n = 12$), measuring fully expanded and illuminated leaf (third from the top), using a portable photosynthesis system LI-6400, outfitted with a leaf chamber fluorometer with 2 cm$^2$ measuring aperture [*LI-COR Biosciences Inc.* 2004]. Leaf temperature was maintained at 25°C. Dark adapted fluorescence measurements and gas exchange parameters were collected before sunrise (at approximately 4:30 A.M.). Light response curves (assimilation rate as function of light level) were collected by ranging incident PAR levels between 0 and 1800 μmol m$^2$ s$^{-1}$, acclimating at each level and maintaining $CO_2$ level slightly above the ambient at 420 ppm. $CO_2$ assimilation responses (assimilation rate as function of intercellular $CO_2$ concentration) were measured ranging $CO_2$ level from 75 to 1500 ppm, acclimating at each level and maintaining incident PAR level at 1600 μmol m$^{-2}$ s$^{-1}$.

## 5. Results

The cotton data set included 160 separate measurements of photosynthetic rate and PAM fluorescence. These were a series of response curves to light, temperature, and $CO_2$ concentration that spanned a range of temperatures from 12 to 40°C, 10 to 600 ppm intercellular $CO_2$, and 0 to 2500 μmol m$^{-2}$ s$^{-1}$ PAR flux. Some experiments were conducted in low (2%) oxygen and others in air. $\Phi_P$ was calculated from fluorescence measurements according to the equation of *Genty et al.* [1989] and from the gas exchange measurements using equation (11). Figure 2a shows a plot of $\Phi_P$ obtained by gas exchange and fluorescence. We also used the data to calibrate the photosynthesis model of *Collatz et al.* [1991]. Simulated and measured rates of photosynthesis are compared in Figure 2b. The model can also be used to simulate $\Phi_P$, and these are compared with the measured values in Figure 2c. These simulations used the default parameter for C3 crops given in *Sellers et al.* [1996] except that $V_{cmo}$ was increased from 100 to 157 μmol m$^{-2}$ s$^{-1}$ and the upper temperature limit parameter ($T_{hi}$) was increased from 308 to 320°K. Our goal is now to extend this model to simulate $\Phi_F$.

As a first step, we plot the observed values of $\Phi_F$ versus $\Phi_P$ (Figure 3) to look for any systematic correlations between the two associated with light levels, $CO_2$ concentration or temperature. While the relationship between $\Phi_F$ and $\Phi_P$ is clearly nonlinear, there is no systematic difference whether changes in $\Phi_F$ are associated with variation in $CO_2$ or light. However, $\Phi_F$ is systematically lower at higher temperatures. The effects of temperature were examined by inspecting the values of $F_o$ and $F_m$ at different temperatures in the cotton and tobacco data (Figure 4). The measurements show a strong decrease of $F_m$ and a weak decrease of $F_o$ when temperature exceeded 26°C. A potential temperature sensitivity of $K_p^o$ or $K_F$
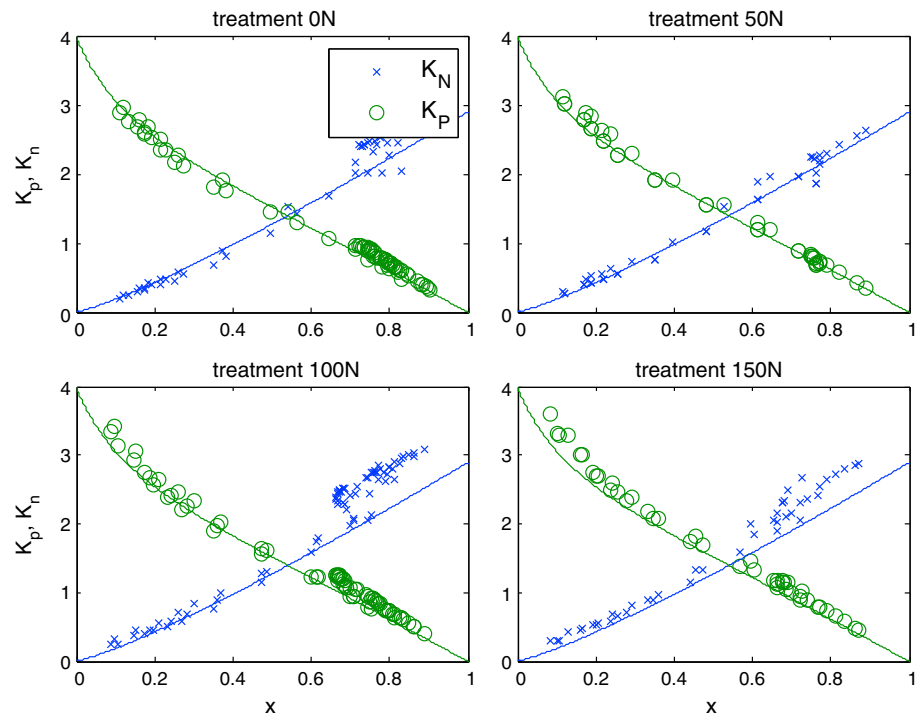
**Figure 7.** Responses of $K_P$ (green) and $K_N$ for four different nitrogen treatments in maize (symbols). The lines represent the empirical fit for the cotton experiment.

alone cannot explain these features. $F_m$ is independent of $K_p^o$, while a temperature sensitivity of $K_F$ would have resulted in nearly equal sensitivity of $F_o$ and $F_m$ to temperature. We attribute the sensitivity to $K_D$, since this can explain the temperature sensitivity of both $F_o$ and $F_m$. A simple temperature correction of $K_D = \max(0.03T + 0.0773, 0.87)$ by means of linear regression above 26°C was sufficient to explain the variations in $F_o$ and $F_m$. $K_D$ also declined at low temperature (10°C in the tobacco data set), but we did not consider the low-temperature values due to the limited number of data points.

The decrease of $F_m$ with temperature is in agreement with observations of *Pospisil et al.* [1998], who observed a decrease of $F_m$ over a much larger temperature range in a Barley (*Hordeum vulgare*) leaf. However, they also observed a progressive increase of $F_o$ starting at 30°C until $F_m$ and $F_o$ collapsed at 50°C. This indicates a decline of $K_p^o$, which we did not observe in the cotton data over the examined temperature range.

## 6. Model for $K_N$

For the cotton data of nondark adapted leaves, we used a constant $K_F$ of 0.05 and the temperature corrected $K_D$ to calculate $K_P$ and $K_N$ (equations (8) and (9)). The relative light saturation $x$ was calculated as follows:

$$x = 1 - \frac{(F'_m - F_t)/F'_m}{(F_m - F_o)/F_m} \qquad (18)$$

A close relationship between the relative light saturation $x$ and $K_N$ was found for the cotton experiment, valid for wide ranges of $CO_2$ concentration and light intensity. Figure 5 shows the two rate coefficients, $K_P$ and $K_N$, and $K_P + K_N$, versus $x$ for this data set. Note that $K_P$ can be considered a dependent variable since $\Phi_P$ and $K_N$ are specified. The dashed line in Figure 5 (top) is the theoretical relationship between $K_P$ and $x$ if $K_N$ were always zero, as in a situation in which NPQ is blocked with an inhibitor *Demmig-Adams* [1990], making the leaf more sensitive to photoinhibition [*Bilger and Björkman*, 1990].

The data of Figure 5 suggest that the relation between $x$ and the rate coefficients can be separated into three parts. At low values of $x$ (<0.2), most of the adjustment of $\Phi_F$ and $\Phi_P$ is done by $K_P$, i.e., reduction of
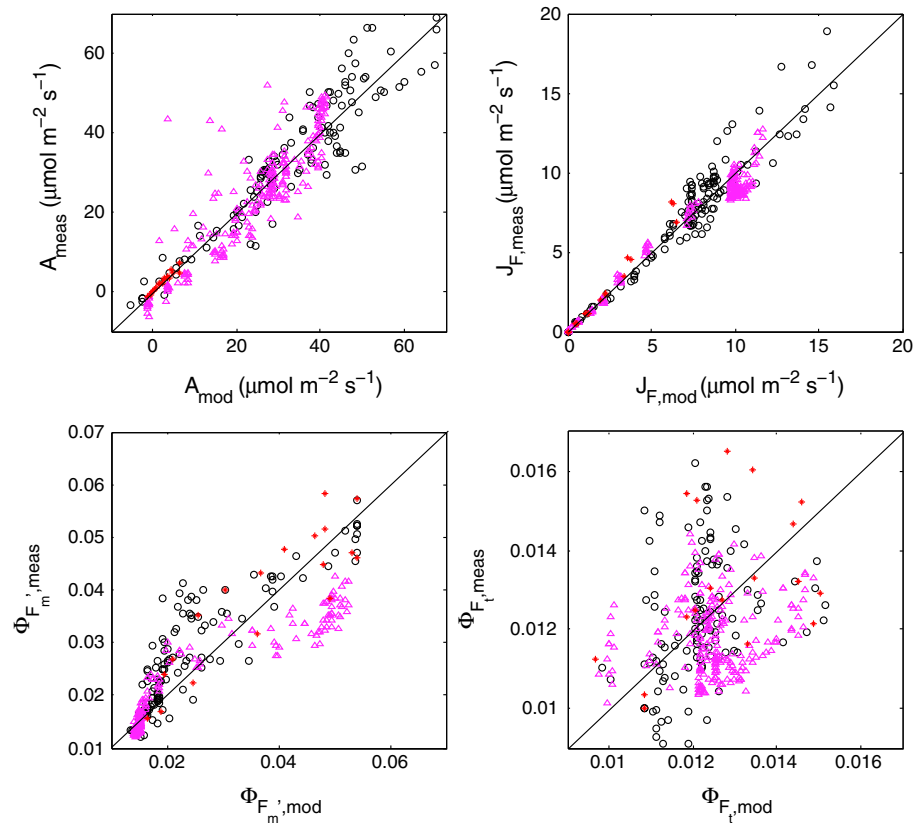
**Figure 8.** Modeled versus measured photosynthesis $A$, fluorescence flux ($\Phi_{F_t} \cdot a$PAR), steady state fluorescence yield $\Phi_{F_t}$, and maximum fluorescence yield $\Phi_{F_m'}$ (clockwise). Circles refer to cotton, triangles to maize, and stars to tobacco.

photosystems, and $K_N$ remains low. At intermediate values ($0.2 < x < 0.6$), there is a phase where $K_P$ stabilizes and most of the adjustment is taken by increasing $K_N$. At the highest values of $x$ ($> 0.6$), the slack is taken up again by decreasing $K_P$. High values of $x$ denote either high irradiance, low-atmospheric $CO_2$ concentration, or high temperature (all these data are plotted together). All data appear to follow the same curve, regardless of which of the driving variables was responsible for the changes in $x$ (excess light, low $CO_2$ concentration, or suboptimal temperatures). Figure 5 (middle), $K_P$ is relatively stable, and thus, variations in the ratio $K_P$:$K_F$ are small. The values in this region correspond to relatively high irradiance: The filled symbols in Figure 5 represent only those data for which $800 < Q < 1800 \, \mu$mol m$^{-2}$ s$^{-2}$ (high light), $14 < T < 35°$C (intermediate temperatures). In those conditions, nonphotochemical quenching dominates, and photochemical yield correlates positively with fluorescence yield.

The relationship between $x$ and $K_N$ was modeled with a curve with three coefficients fitted to the data (solid line in Figure 5), using all data where leaf temperature was between 14 and 35°C:

$$K_N = \nu K_N^o \quad \text{with} \quad \nu = \frac{(1 + \beta)x^\alpha}{\beta + x^\alpha} \tag{19}$$

where $K_N^o$, $\alpha$, and $\beta$ are fitting parameters. The form of this equation was chosen to obtain $K_N = K_N^o$ for $x = 1$ and $K_N = 0$ for $x = 0$ and values in between these extremes for $0 < x < 1$. Fitting by means of minimization of the mean square difference between measured and modeled $K_N$ resulted in $K_N^o = 2.48$, $\alpha = 2.83$, and $\beta = 0.114$.

Data of the other experiments C3 species were plotted in the same way (rate coefficients versus $x$) in Figure 6. Interestingly, light and $CO_2$ response curves of the tobacco experiment were similar to those of the cotton experiment despite having very different photosynthetic capacities. Apparently, the approach of scaling the quenching response to the $x$ factor can accommodate differences in photosynthetic rate. Interestingly, data for the C4 plant maize followed a similar pattern to cotton and tobacco (Figure 7). There
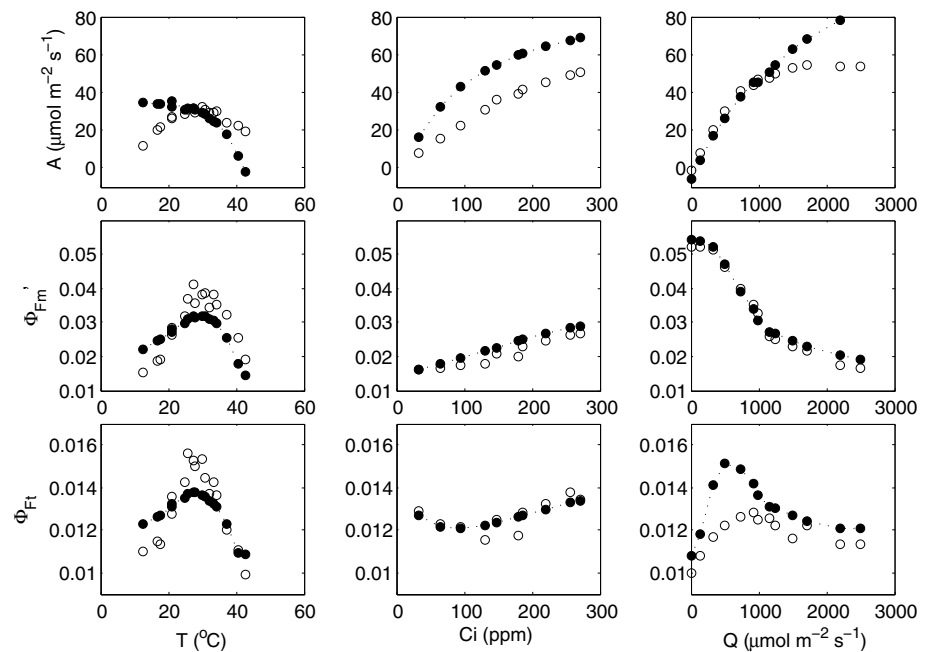
**Figure 9.** Measured (open symbols) and modeled (closed symbols) responses of photosynthesis, maximum fluorescence yield, and steady state fluorescence yield of selected cotton leaves to temperature, leaf boundary layer $CO_2$ concentration, and irradiance.

was no apparent difference in the $K_N$ versus $x$ relation for leaves from different nitrogen fertilization treatments, despite having nearly 50% differences in carboxylation capacity at optimum temperature, $V_{cmo}$. On the other hand, data of the drought experiment, where measurements were taken outdoors on several drought-adapted plants at similar light intensity, deviated from the other observations at higher values of $x$. Instead of a curve with $K_N$ reaching a maximum around 2.5, $K_N$ continues to increase with increasing $x$ to about 5. Apparently, NPQ traps a larger portion of excited states under sustained drought conditions. Consequently, the fraction of closed photosystems at a given value of $x$ is smaller (and $K_P$ is higher) than in the experiments without water limitation (cotton, maize, and tobacco). We note that the cotton, maize, and tobacco plants had little or no previous exposure to stress and may not be representative of vegetation in natural environments. The values for the drought experiment were sufficiently different from the other experiments to justify a separate fit of equation (19) through the $K_N$ versus $x$ data, with coefficients $K_N^o = 5.01$, $\alpha = 1.93$, and $\beta = 10$.

We are now in a position to link this paramaterization with the photosynthesis model. As shown Figure 2c, $\Phi_P$ simulated with the carbon model agrees well with the corresponding observations. Similar results were obtained with tobacco and using the C4 model of *Collatz et al.* [1992]. Thus, we may evaluate the parameter $x$ that corresponds to any model calculation of photosynthesis from the ratio $\Phi_P/\Phi_P^o$ calculated in the solution to the carbon model. It is important that the two yields used to evaluate $x$ are consistent such that $x \rightarrow 0$ in the limit as PAR $\rightarrow 0$. $K_N$ can then be evaluated using equation (19) and used in equation (13) to solve for $\Phi_{F_m'}$ which in turn is used in equation (17) to solve for our target, $\Phi_{F_t}$. Note that the $\Phi_P^o$ used in equation (17) should be from the fluorescence rather than from the carbon model.

Figure 8 shows measured versus modeled photosynthesis $A$, $\Phi_{F_m'}$, and $\Phi_{F_t}$ after fitting the model of *Collatz et al.* [1991] to the cotton and the tobacco and the model of *Collatz et al.* [1992] to the maize data. Also shown in this figure is the product of $\Phi_{F_t}$ and the flux of absorbed PAR, $J_{aPAR}$ (estimated assuming that $J_{aPAR} = 0.9 \cdot Q/2$ where 0.9 is the absorptance and $Q$ is the incident flux). This is an approximation for the fluorescence flux emitted by the leaf $J_F$. In each case the model was calibrated to the respective data sets (e.g., all cotton points), and the same parameter set was used to simulate the group of observations. The model reproduces the photosynthesis and maximum fluorescence $\Phi_{F_m'}$ reasonably well. However, the simulations of the fluorescence yield $\Phi_{F_t}$ are poorly correlated. In part, this is due to the very small variation ($\pm25\%$) in $\Phi_{F_t}$ observed in the experiment and to errors in measurement of these small differences. It should
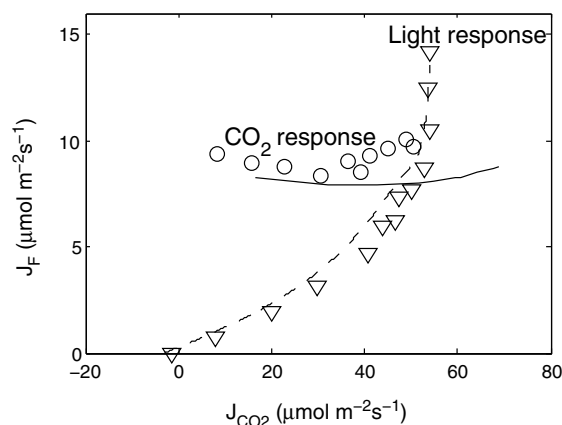
**Figure 10.** Selection of the cotton data for one light response curve (triangles) and one $CO_2$ response curve at an incident PAR of 1400 $\mu$mol m$^{-2}$ s$^{-1}$ (circles), with $CO_2$ gas exchange flux on the horizontal axis and fluorescence flux $J_P = \Phi_P \cdot a\text{PAR}/2$ from PAM data on the vertical axis. The lines are model results (cotton parameters for $K_N(x)$) after coupling the PAM fluorescence model to the model of *Collatz et al.* [1991].

also be noted that other factors such as photoinhibition [*Demmig-Adams and Adams III*, 1996] or chloroplast movement [*Brugnoli and Bjorkman*, 1992] may also cause changes in the apparent $\Phi_{F_t}$. We did not control for these.

Despite the poor overall performance of the model to reproduce $\Phi_{F_t}$, mainly due to its low variability, simulated versus modeled responses of cotton to environmental drivers light, $CO_2$, and temperature compare well with observations (Figure 9). Of particular interest is the sensitivity to temperature, as illustrated in Figure 9. The model did not capture the temperature sensitivity of photosynthesis well, especially at the lower and higher temperatures, where it overestimates photosynthesis, and hence $x$. It appears that this is primarily due to calibration errors of the photosynthesis model and fluorescence modeling may be useful to identify and correct problems with model calibration.

If we consider Figure 8 again, we can observe that contrary to $\Phi_{F_t}$, the fluorescence flux $J_F$ is reproduced well. The reason is the small range in $\Phi_{F_t}$ and the dominant effect that incident light flux has on $J_F$. The dominance of irradiance on $J_F$ is further illustrated in Figure 10, showing a selection of modeled and "measured" $J_F$ as $\Phi_{F_t} \cdot J_{a\text{PAR}}$ versus the $CO_2$ flux from gas exchange for the cotton data. The selection consists of a light response and a $CO_2$ response curve. The light response shows the combined effect of variations in $J_{a\text{PAR}}$ and the yields, whereas the $CO_2$ response is only affected by variations in the yields ($J_{a\text{PAR}}$ was constant). With irradiance as the driving variable, we notice a large range of fluorescence flux, continuing to increase even after $J_A$ saturates. The variations in fluorescence flux are much smaller when $CO_2$ is the driving variable. In that case, all variation of the fluorescence flux originates from the fluorescence yield, while $a\text{PAR}$ was constant. In either case, the simulations tracked the observations well.

## 7. Discussion

We have developed an extension of a conventional photosynthesis model to simulate fluorescence. We used an empirical approach to relate NPQ to a factor, $x$, that expresses the extent to which the actual rate of electron transport is reduced relative to the potential rate. This relationship is similar whether variation is driven by manipulation of light, $CO_2$, and carboxylation capacity. Here we used the photosynthesis models of *Collatz et al.* [1991] for C3 and *Collatz et al.* [1992] for C4 vegetation, but this approach could be used by any model based on the assumptions of *Farquhar et al.* [1980]. A one-by-one sensitivity analysis of this combined fluorescence-photosynthesis model revealed that $a\text{PAR}$ and the carboxylation capacity $V_{cmo}$ are main contributors to variations in fluorescence yield and that their contributions are comparable in magnitude (Figure 11). Temperature affects the dark reactions of photosynthesis [*Weis and Berry*, 1987b], with an additional effect of $K_D$ being temperature dependent. Stomatal effects mediated by the relative humidity appear to have a relatively small effect on fluorescence yield, except at low relative humidity.

In Figure 12 we show how changes in fluorescence yield associated with changes in $V_{cmo}$, which might occur during drought or senescence, correspond to changes in the fluorescence intensity, $J_F$. For this figure drought parameters for $K_N$ versus $x$ were used. Changing $V_{cmo}$ affects the value of irradiance at which the peak of the fluorescence yield occurs (Figure 12, top left). The peak occurs at the transition from light limited to light-saturated photosynthesis, where neither light nor $CO_2$ is in deficit. The fluorescence *yield* thus peaks at a $V_{cmo}$-dependent irradiance, but the fluorescence *flux* continuously rises with irradiance (Figure 12, bottom left). The rise in intensity is initially steep, but it flattens after the peak of fluorescence yield. Hence, the transition point between light limitation and light saturation can be derived from the change in slope
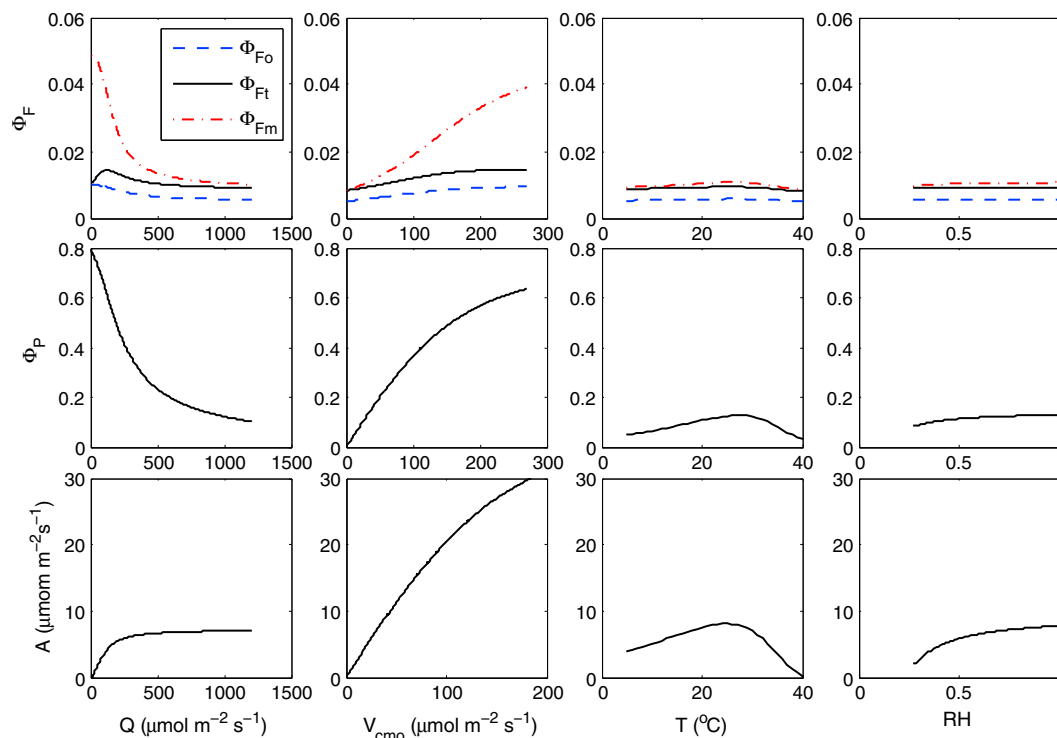
**Figure 11.** One-by-one sensitivity analysis of the modeled yields (fluorescence and photochemistry) and photosynthesis of a "standard" leaf to four input variables. The sensitivity was calculated for drought relation between $x$ and $K_N$. The parameters of the standard leaf were leaf boundary $[CO_2]$ = 380 ppm, $a$PAR = 1000 μmol m$^{-2}$s$^{-1}$, leaf temperature $T$ = 20°C, relative humidity RH = 70%, $V_{cmo}$ = 30 μmol m$^{-2}$ s$^{-1}$, and Ball-Berry stomatal conductance parameter $m$ = 8.
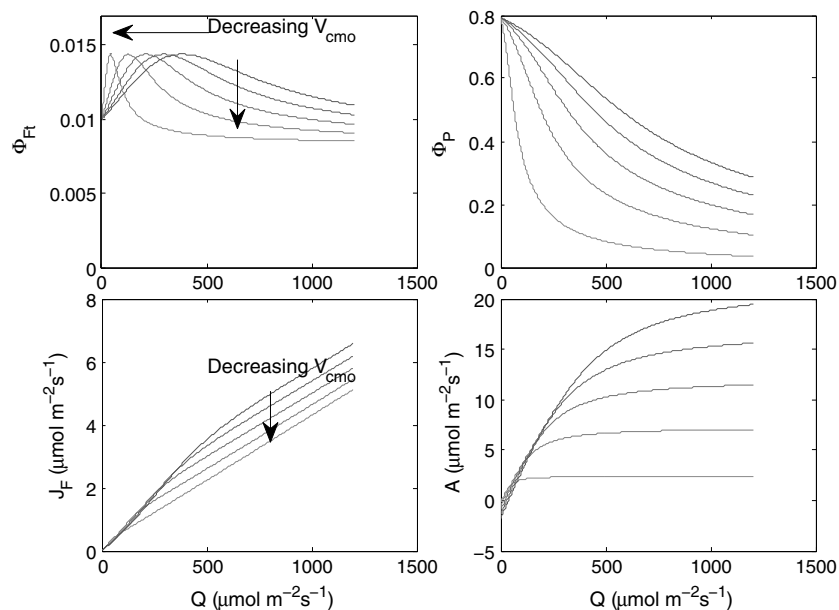


**Figure 12.** (top left) Modeled fluorescence yield $\Phi_{Ft}$ (top right) photochemical yield $\Phi_P$, (bottom left) photosynthesis $A$, and (bottom right) fluorescence flux $J_F$, as functions of irradiance for the following values of maximum carboxylation capacity $V_{cmo}$: 10 (light gray), 30, 50, 70, and 90 (black) μmol m$^{-2}$ s$^{-1}$. The drought relation between $x$ and $K_N$ was used.
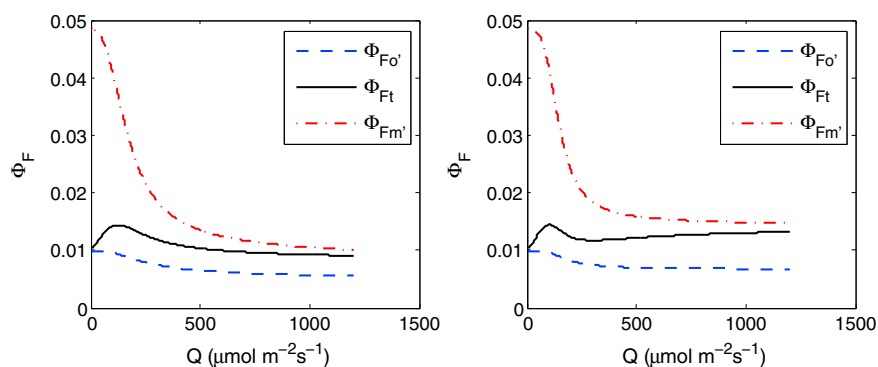
**Figure 13.** Modeled responses of $\Phi_{Fm'}$, $\Phi_{Fo'}$, and $\Phi_F$ to irradiance, (left) using the drought parameters for $K_N(x)$ and (right) using the cotton parameters for $K_N(x)$.

between the fluorescence flux and irradiance. The photochemical yield (Figure 12, top right) decreases strongly with irradiance, as the rate of $CO_2$ uptake begins to saturate (Figure 12, bottom right).

A clearly different response between the light, $CO_2$, and fertilization experiments on one hand, and the drought experiment on the other hand, prevents us from presenting a deterministic model for $K_N$ for all cases. The differences in $K_N$ values at high $x$ between the two model fits have a number of implications for the sensitivity of the model and for the interpretation of fluorescence yields, as illustrated in Figure 13. When the parameters of the cotton data are used, then $K_N$ levels off and $\Phi_{F_t}$ increases at the highest values of $x$ (stressed conditions). This is illustrated in Figure 13 (right), where the yields were modeled using the cotton $K_N(x)$ parameterization as a function of irradiance. The steady state yield first increases, then decreases, and finally increases with irradiance. In the drought experiment, values of $\Phi_F$ continue to decrease with irradiance (Figure 13, left), and the lowest fluorescence yields indicate stress.

The mechanisms of NPQ and their regulation are still an area of active research (for reviews see *Ruban et al.* [2012] and *Zaks et al.* [2013]). We speculate that the shape of the $x$-$K_N$ relationship is affected by xanthophyll pool sizes as influenced by adaptation to weather conditions. A practical approach would be to relate $K_N^o$ to the concentration of pigments that are capable of NPQ [*Lavergne and Trissl*, 1995; *Oxborough and Baker*, 2000]. As noted by *Zaks et al.* [2013], a high zeaxanthin concentration is necessary but not sufficient for non-photochemical quenching. To study this further, active fluorescence measurements should be combined with concurrent spectrometry, while tapping into earlier studies that showed a photochemical reflectance index correlating with xanthophyll pigment conversions [*Gamon et al.*, 1990].

The analysis presented here have been made for the leaf level. We did not present any canopy level analyses here, although we have implemented the model the 'Soil Canopy Observation of Photosynthesis and Energy fluxes (SCOPE) model, [*van der Tol et al.*, 2009b]. In the canopy, leaf illumination is variable among leaves, and the relationship after aggregating over all leaves may differ from what we presented here. In addition, the emitted fluorescence flux is scattered and reabsorbed within the canopy, thus reducing the observed SIF below the emitted flux of all leaves together. We expect, however, that some features of the leaf level photosynthesis-SIF relationship remain because any observation from the top of canopy will be dominated by the top and most illuminated leaves. First, that NPQ is the main driver of variations in $\Phi_P$ and $\Phi_{F_t}$ and that the two yields are positively related during daytime. Variations in canopy measurements of SIF, after normalization by estimates of the absorbed PAR, may be related to drought or temperature stress. Second, the variations in $\Phi_{F_t}$ are small compared to those in $\Phi_P$ (Figure 3). In spatial SIF data (airborne and satellite data) over terrain of mixed vegetation, variations in photosynthetically active leaf area (green leaf area index) will most likely dominate the variations in SIF, since these variations may be much larger than the variations in $\Phi_{F_t}$ that we observed here.

## 8. Conclusion

The fluorescence yield of leaves is strongly influenced by the development of nonphotochemical quenching (NPQ). This (and not fluorescence) is the predominant mechanism for dissipation of excess excitation energy. In fact, fluorescence yield typically remains nearly constant or declines as a result of increased NPQ

when leaves experience over excitation. We introduce a factor $x$ that indicates the relative extent that photochemistry of photosystem II is restricted by the limited capacity for $CO_2$ fixation, and we show that there is a strong empirical relationship between the rate constant for nonphotochemical quenching, $K_N$, and $x$. While this relationship may differ with species and history, it is easily characterized with PAM fluorescence measurements. The other important determinant of fluorescence yield, $K_P$, is captive to the level of $K_N$ and the permitted rate of electron transport under light saturation or stress due to strong limitations on photosynthesis by other factors than light. The empirical fits of $K_N$ versus $x$ can be used in combination with a photosynthesis model to estimate leaf level fluorescence yield as a function of environmental forcing and photosynthetic capacity. Estimation of the flux of leaf level solar-induced fluorescence (SIF) from the predicted fluorescence yields (Figure 12) shows that SIF will be proportional to photosynthetic rate under conditions where light is limiting. When light is in excess or stress develops, there is a reduction in the fluorescence yield and the slope of the dependence of SIF on light intensity declines. This is the basis for inversions to obtain $V_{cmo}$ [*Zhang et al.*, 2014]. With increasing stress or reductions in $V_{cmo}$ at constant light (as would occur with repeated Sun-synchronous satellite observations), SIF would be observed to decrease. The extent of this decrease may depend on the severity and type of stress.

# References

Bilger, W., and O. Björkman (1990), Role of the xanthophyll cycle in photoprotection elucidated by measurements of light-induced absorbance changes, fluorescence and photosynthesis in leaves of Hedera canariensis, *Photosynth. Res.*, *25*(3), 173–185.

Bilger, W., U. Schreiber, and M. Bock (1995), Determination of the quantum efficiency of photosystem II and of non-photochemical quenching of chlorophyll fluorescence in the field, *Oecologia*, *102*(4), 425–432.

Björkman, O., and B. Demmig (1987), Photon yield of $O_2$ evolution and chlorophyll fluorescence characteristics at 77 K among vascular plants of diverse origins, *Planta*, *170*(4), 489–504.

Brugnoli, E., and O. Bjorkman (1992), Chloroplast movements in leaves: Influence on chlorophyll fluorescence and measurements of light-induced absorbance changes related to Δph and zeaxanthin formation, *Photosynth. Res.*, *32*(1), 23–35, doi:10.1007/BF00028795.

Butler, W. L. (1978), Energy distribution in the photochemical apparatus of photosynthesis, *Ann. Rev. Plant Physiol.*, *29*(1), 345–378.

Collatz, G., J. Ball, C. Grivet, and J. A. Berry (1991), Physiological and environmental regulation of stomatal conductance, photosynthesis and transpiration: A model that includes a laminar boundary layer, *Agric. Forest Meteorol.*, *54*(2–4), 107–136, doi:10.1016/0168-1923(91)90002-8.

Collatz, G., M. Ribas-Carbo, and J. Berry (1992), Coupled photosynthesis-stomatal conductance model for leaves of $C_4$ plants, *Funct. Plant Biol.*, *19*(5), 519–538.

Daughtry, C. S. (2001), Discriminating crop residues from soil by shortwave infrared reflectance, *Agron. J.*, *93*(1), 125–131.

Demmig-Adams, B. (1990), Carotenoids and photoprotection in plants: A role for the xanthophyll zeaxanthin, *Biochim. Biophys. Acta, Bioenerg.*, *1020*(1), 1–24.

Demmig-Adams, B., and W. W. Adams III (1996), The role of xanthophyll cycle carotenoids in the protection of photosynthesis, *Trends Plant Sci.*, *1*(1), 21–26.

Farquhar, G., S. v. v. Caemmerer, and J. Berry (1980), A biochemical model of photosynthetic $CO_2$ assimilation in leaves of $C_3$ species, *Planta*, *149*(1), 78–90.

Fleming, G. R., G. S. Schlau-Cohen, K. Amarnath, and J. Zaks (2012), Design principles of photosynthetic light-harvesting, *Faraday Discuss.*, *155*, 27–41.

Flexas, J., J. Escalona, and H. Medrano (1998), Down-regulation of photosynthesis by drought under field conditions in grapevine leaves, *Funct. Plant Biol.*, *25*(8), 893–900.

Flexas, J., J. M. Escalona, S. Evain, J. Gulías, I. Moya, C. B. Osmond, and H. Medrano (2002), Steady-state chlorophyll fluorescence (Fs) measurements as a tool to follow variations of net $CO_2$ assimilation and stomatal conductance during water-stress in $C_3$ plants, *Physiol. Plant.*, *114*(2), 231–240.

Franck, F., P. Juneau, and R. Popovic (2002), Resolution of the Photosystem I and Photosystem II contributions to chlorophyll fluorescence of intact leaves at room temperature, *Biochim. Biophys. Acta, Bioenerg.*, *1556*(2), 239–246.

Frankenberg, C., et al. (2011), New global observations of the terrestrial carbon cycle from GOSAT: Patterns of plant fluorescence with gross primary productivity, *Geophys. Res. Lett.*, *38*, L17706, doi:10.1029/2011GL048738.

Gamon, J., C. Field, W. Bilger, O. Björkman, A. Fredeen, and J. Peñuelas (1990), Remote sensing of the xanthophyll cycle and chlorophyll fluorescence in sunflower leaves and canopies, *Oecologia*, *85*(1), 1–7.

Genty, B., J.-M. Briantais, and N. R. Baker (1989), The relationship between the quantum yield of photosynthetic electron transport and quenching of chlorophyll fluorescence, *Biochim. Biophys. Acta, Bioenerg.*, *990*(1), 87–92, doi:10.1016/S0304-4165(89)80016-9.

Gilmore, A. M. (1997), Mechanistic aspects of xanthophyll cycle-dependent photoprotection in higher plant chloroplasts and leaves, *Physiol. Plant.*, *99*(1), 197–209.

Guanter, L., L. Alonso, L. Gómez-Chova, J. Amorós-López, J. Vila, and J. Moreno (2007), Estimation of solar-induced vegetation fluorescence from space measurements, *Geophys. Res. Lett.*, *34*, L08401, doi:10.1029/2007GL029289.

Hildner, R., D. Brinks, J. B. Nieder, R. J. Cogdell, and N. F. van Hulst (2013), Quantum coherent energy transfer over varying pathways in single light-harvesting complexes, *Science*, *340*(6139), 1448–1451, doi:10.1126/science.1235820.

Joiner, J., Y. Yoshida, A. P. Vasilkov, Y. Yoshida, L. A. Corp, and E. M. Middleton (2011), First observations of global and seasonal terrestrial chlorophyll fluorescence from space, *Biogeosciences*, *8*(3), 637–651, doi:10.5194/bg-8-637-2011.

Kitajima, M., and W. Butler (1975), Quenching of chlorophyll fluorescence and primary photochemistry in chloroplasts by dibromothymoquinone, *Biochim. Biophys. Acta, Bioenerg.*, *376*(1), 105–115, doi:10.1016/0005-2728(75)90209-1.

Lavergne, J., and H.-W. Trissl (1995), Theory of fluorescence induction in photosystem II: Derivation of analytical expressions in a model including exciton-radical-pair equilibrium and restricted energy transfer between photosynthetic units, *Biophys. J.*, *68*(6), 2474–2492.

LI-COR Biosciences Inc. (2004), Using the LI-6400 Portable Photosynthesis System, Version 5, *Tech. Rep. 9806-122*, LI-COR Biosciences Inc., Lincoln, Nebr.

Loriaux, S., T. Avenson, J. Welles, D. McDermitt, R. Eckles, B. Riensche, and B. Genty (2013), Closing in on maximum yield of chlorophyll fluorescence using a single multiphase flash of sub-saturating intensity, *Plant Cell Environ.*, *36*(10), 1755–1770.

Markgraf, T., and J. Berry (1990), Measurement of photochemical and non-photochemical quenching: Correction for turnover of $PS_2$ during steady-state photosynthesis, in *Current Research in Photosynthesis*, pp. 3073–3076, Springer, Netherlands.

Maxwell, K., and G. Johnson (2000), Chlorophyll fluorescence—A practical guide, *J. Exp. Bot.*, *51*(345), 1–10.

Mazzoni, M., M. Meroni, C. Fortunato, R. Colombo, and W. Verhoef (2012), Retrieval of maize canopy fluorescence and reflectance by spectral fitting in the $O_2$-A absorption band, *Remote Sens. Environ.*, *124*, 72–82.

Meroni, M., M. Rossini, L. Guanter, L. Alonso, U. Rascher, R. Colombo, and J. Moreno (2009), Remote sensing of solar-induced chlorophyll fluorescence: Review of methods and applications, *Remote Sens. Environ.*, *113*(10), 2037–2051, doi:10.1016/j.rse.2009.05.003.

Mohseni, M., P. Rebentrost, S. Lloyd, and A. Aspuru-Guzik (2008), Environment-assisted quantum walks in photosynthetic energy transfer, *J. Chem. Phys.*, *129*(174,106), doi:10.1063/1.3002335.

Moya, I., L. Camenen, S. Evain, Y. Goulas, Z. Cerovic, G. Latouche, J. Flexas, and A. Ounis (2004), A new instrument for passive remote sensing: 1. Measurements of sunlight-induced chlorophyll fluorescence, *Remote Sens. Environ.*, *91*(2), 186–197, doi:10.1016/j.rse.2004.02.012.

Oxborough, K., and N. R. Baker (2000), An evaluation of the potential triggers of photoinactivation of photosystem II in the context of a Stern-Volmer model for downregulation and the reversible radical pair equilibrium model, *Philos. Trans. R. Soc. B*, *355*(1402), 1489–1498.

Papageorgiou, G. C., et al. (2004), *Chlorophyll a Fluorescence: A Signature of Photosynthesis*, vol. 19, Springer, Netherlands.

Porcar-Castell, A., E. Tyystjärvi, J. Atherton, C. van der Tol, J. Flexas, E. E. Pfündel, J. Moreno, C. Frankenberg, and J. A. Berry (2014), Linking chlorophyll a fluorescence to photosynthesis for remote sensing applications: Mechanisms and challenges, *J. Exp. Bot.*, *65*, 4065–4095, doi:10.1093/jxb/eru191.

Pospisil, P., J. Skotnica, and J. Naus (1998), Low and high temperature dependence of minimum $F_0$ and maximum $F_m$ chlorophyll fluorescence in vivo, *Biochim. Biophys. Acta, Bioenerg.*, *1363*(2), 95–99.

Rebentrost, P., M. Mohseni, and A. Aspuru-Guzik (2009), Role of quantum coherence and environmental fluctuations in chromophoric energy transport, *J. Phys. Chem. B.*, *113*(29), 9942–9947, doi:10.1021/jp901724d.

Ruban, A. V., M. P. Johnson, and C. D. Duffy (2012), The photoprotective molecular switch in the photosystem II antenna, *Biochim. Biophys. Acta, Bioenerg.*, *1817*(1), 167–181.

Schreiber, U., U. Schliwa, and W. Bilger (1986), Continuous recording of photochemical and non-photochemical chlorophyll fluorescence quenching with a new type of modulation fluorometer, *Photosynth. Res.*, *10*(1–2), 51–62.

Sellers, P., D. Randall, G. Collatz, J. Berry, C. Field, D. Dazlich, C. Zhang, G. Collelo, and L. Bounoua (1996), A revised land surface parameterization (SiB2) for atmospheric GCMSs. Part I: Model formulation, *J. Clim.*, *9*(4), 676–705.

van der Tol, C., W. Verhoef, and A. Rosema (2009a), A model for chlorophyll fluorescence and photosynthesis at leaf scale, *Agric. Forest Meteorol.*, *149*(1), 96–105.

van der Tol, C., W. Verhoef, J. Timmermans, A. Verhoef, and Z. Su (2009b), An integrated model of soil-canopy spectral radiances, photosynthesis, fluorescence, temperature and energy balance, *Biogeosciences*, *6*(12), 3109–3129, doi:10.5194/bg-6-3109-2009.

Weis, E., and J. A. Berry (1987a), Quantum efficiency of photosystem II in relation to energy-dependent quenching of chlorophyll fluorescence, *Biochim. Biophys. Acta, Bioenerg.*, *894*(2), 198–208, doi:10.1016/0005-2728(87)90190-3.

Weis, E., and J. A. Berry (1987b), Plants and high temperature stress, *Symp. Soc. Exp. Biol.*, *42*, 329–346.

Woodrow, I., and J. Berry (1988), Enzymatic regulation of photosynthetic $CO_2$ fixation in C-3 plants, *Annu. Rev. Plant Physiol. Plant Mol. Biol*, *39*, 533–594, doi:10.1146/annurev.arplant.39.1.533.

Zaks, J., K. Amarnath, E. J. Sylak-Glassman, and G. R. Fleming (2013), Models and measurements of energy-dependent quenching, *Photosynt. Research*, *116*(2-3), 389–409.

Zarco-Tejada, P., A. Catalina, M. González, and P. Martín (2013), Relationships between net photosynthesis and steady-state chlorophyll fluorescence retrieved from airborne hyperspectral imagery, *Remote Sens. Environ.*, *136*, 247–258, doi:10.1016/j.rse.2013.05.011.

Zhang, Y., L. Guanter, J. A. Berry, J. Joiner, C. Tol, A. Huete, A. Gitelson, M. Voigt, and P. Köhler (2014), Estimation of vegetation photosynthetic capacity from space-based measurements of chlorophyll fluorescence for terrestrial biosphere models, *Global Change Biol.*, *20*(12), 3727–3742.